ARTICLE

Identification of Intermediates in Pyridine Pyrolysis with Molecular-beam Mass Spectrometry and Tunable Synchrotron VUV Photoionization†

Xin Hong, Tai-chang Zhang, Li-dong Zhang, Fei Qi*

National Synchrotron Radiation Laboratory, University of Science and Technology of China, Hefei 230029, China

(Dated: Received on March 6, 2009; Accepted on March 17, 2009)

The pyrolysis of pyridine (5.26% pyridine in argon) was performed with tunable synchrotron vacuum ultraviolet photoionization and molecular-beam mass spectrometry technique at the temperature range of 1255-1765 K at 267 Pa. About 20 products and intermediates, containing major species H_2, HCN, C_2H_2, C_5H_3N, C_4H_2, and C_3H_3N, were identified by near-threshold measurements of photoionization mass spectra and their mole fractions *vs.* temperatures were estimated. The major reaction pathways are analyzed based on the experimental observations.

Key words: Pyridine pyrolysis, Intermediate, Tunable synchrotron VUV photoionization, Molecular-beam mass spectrometry

I. INTRODUCTION

Pyridine, the simplest six-membered heterocyclics, is the model and representative of nitrogen-containing compounds in the coal and coal-derived fuels [1-4], whose combustion leads to the NO_x emission [5-7]. The pyrolysis of pyridine occurs in the pre-flame zone or during the initial heat-up period of the fuel prior to combustion [8,9], therefore the identification of the pyrolysis intermediates and quantitative determination are helpful for further understanding of the evolution of NO_x [10].

The thermal decomposition of pyridine has been extensively studied. Hydrogen, acetylene and hydrogen cyanide were detected as the major pyrolysis products, along with minor components such as acrylonitrile (C_3H_3N), benzonitrile(C_7H_5N), and methane in flow systems at the temperature range of 950-1400 K [10,11]. Shock tube pyrolysis of pyridine shows major products (C_2H_2, HCN, C_3HN, and H_2) and minor ones vinylacetylene (C_4H_4), cycanovinylacetylene (C_5H_3N), and diacetylene (C_4H_2) at a rather high temperature range of 1200-1800 K [12,13]. As reported previously, HCN appears to be the key nitrogen-containing intermediate formed during the pyrolysis of this heterocyclic compound, however, some difference existed in the identification of some major and minor pyrolysis products, especially for acetonitrile (C_2H_3N) [10] and cyanoacetylene (C_3HN) [14]. It is noticeable that in previous investigations it has been difficult to identify radicals and isomeric species using electron-impact ionization mass spectrometry (EIMS) and/or gas chromatography (GC) due to the limited energy resolution of ionizing electrons and fragmental interference of EIMS, and the characteristics of the GC method.

In this work, molecular-beam mass spectrometric technique coupled with tunable synchrotron VUV photoionization method was applied to the pyrolysis investigation of pyridine to comprehensively determine the pyrolysis intermediates. This method has been adopted to identify the intermediates in combustion, especially radicals and isomers, by reducing fragmentation via near-threshold photoionization [15-17]. Moreover the mole fraction profiles and the schematics of the products formation are also provided in this work.

II. EXPERIMENTS

The experiment was carried out at the National Synchrotron Radiation Laboratory (NSRL) in Hefei, China. A detailed description of the instrument setup has been reported elsewhere [18], and only a brief description is presented here. An undulator radiation from the 800 MeV electron storage ring is dispersed by a 1 m Seya-Namioka monochromator with a 1.50 groove/m laminar grating covering the photon energy range from 7.80 eV to 24.00 eV. The energy resolving power is approximately 10^3. The average photon flux can reach the magnitude of 10^{13} photon/s. A gas filter is used to eliminate higher-order harmonic radiation with Ne or Ar filled in the gas cell for this work. The apparatus is composed of a pyrolysis chamber equipped with a high temperature furnace, a differentially pumped chamber with a molecular-beam sampling system, and a photoioniza-

†Part of the special issue for "the 4th Sino-French Workshop on Molecular Spectroscopy, Dynamics and Quantum Control".

*Author to whom correspondence should be addressed. E-mail: fqi@ustc.edu.cn, FAX: +86-551-5141078, Tel.: +86-551-3602125

tion chamber with a reflection time-of-flight mass spectrometer (RTOF-MS). Pyridine was controlled by a syringe pump (ISCO 1000D) with the liquid flow rate of 0.10 mL/min (equivalent to 27.75×10^{-3} SLM in gas phase) at room temperature. Subsequently, pyridine was vaporized and mixed with Ar which was controlled by a MKS mass flow controller with the flow rate of 0.50 SLM. The vaporizer was kept at a temperature of 450 K. Then the mixture of pyridine and Ar was fed into a 3.0-mm-ID (inside diameter) and 300-mm length alumina flow tube with 60 mm stationed inside the furnace. The pyrolysis species, including the reactant, intermediates, and products, were sampled by a quartz nozzle with a ∼500 μm orifice at the tip. The formed molecular-beam in the differentially pumped chamber then passed into the photoionization chamber through a nickel skimmer and was crossed by the tunable synchrotron VUV light. A digital delay generator (DG 535, SRS) was used to trigger a pulsed power supply and the multiscaler (P7888, FAST Comtec) as well. The ions were drawn out of the photoionization region by the pulse extraction field and subsequently collected by a microchannel plate (MCP) detector. Finally the signal was recorded by the multiscaler via a preamplifier VT120C (EG&G, ORTEC). A silicon photodiode (SXUV-100, International Radiation Detectors, Inc.) was used to monitor the photon flux for normalizing ion signals. Pyridine was purchased from Sinopharm Chemical Reagent Limited Co., Shanghai, China with a purity of ≥99.5%. No further purification was performed for this study.

To reduce collisions of the pyrolysis species and detect the primary and secondary products including radicals, the pyrolysis chamber was kept at low pressure (267 Pa) controlled by a MKS throttle valve in this work. The temperature was measured by a Pt-30%Rh/Pt-6%Rh thermocouple inserted in the heating region inside the flow tube. The temperature uncertainty is within 50 K.

A series of mass spectra were measured with the variation of photon energy at specified temperature for measurements of photoionization efficiency (PIE) spectra. The integrated ion intensities for a specified mass were normalized by the photon flux and then plotted as a function of the photon energy, which yielded PIE spectra containing information of ionization energies (IEs) of specific species. Mass spectra can also be recorded at fixed photon energy for various pyrolysis temperatures. In order to avoid fragmentation, mass spectra were recorded at near-ionization thresholds for temperature scanning. In this work, the measurements were carried out at the selected photon energies of 16.00, 11.70, 11.00, 10.78, 10.00, and 9.50 eV. The temperature ranged from 1255 K to 1765 K.

III. RESULTS AND DISCUSSION

A. Species Identification

The identification of pyrolysis species is based on the measurement of photoionization mass spectra and the photoionization efficiency spectra (PIE). A stack plot of photoionization mass spectra within the temperature range of 1255-1765 K is presented in Fig.1. The selected energy is 11.70 eV, at which most of the pyrolysis intermediates and products can be ionized and detected. Partial signals are amplified by a factor of 4 in order to clearly reveal the weak peaks. The intensities of pyrolysis intermediates and products varies as the temperature increases. The amount of pyridine decreases to about 25% at 1765 K.

A stack plot of photoionization mass spectra of pyridine with four different photon energies ranging from 9.50 eV to 16.00 eV at 1745 K is presented in Fig.2. Part of the mass spectra (from m/z=88 to 110) are amplified by a factor of 2 for the better illustration of the mass peaks of m/z=103 and 104. Mass peaks of m/z=52, 74 can be recognized together with trace amount of m/z=53, 54, 78, and 103 at the energies lower than 11.00 eV. As the energy increases, the peaks become abundant which correspond to most of the pyrolysis intermediates and products, such as m/z=28, 40, 50, 65, 77, 79. Specially, m/z=26, 53 and trace amount of m/z=51 began to emerge at energy higher than 11.70 eV. The mass peaks of m/z=16 and 27 can be observed at the high energy of 16.00 eV. Furthermore, the identification of pyrolysis species can be obtained by the further measurement of PIE spectra which are selectively depicted in Fig.3. Clear onsets on PIE spectra of m/z=26 and 51 are located at 11.40 and 11.61 eV, as shown in Fig.3, which correspond to the IEs of acetylene (11.40 eV [19]) and cyanoacetylene (11.61 eV [19]), respectively. In this work, about 20

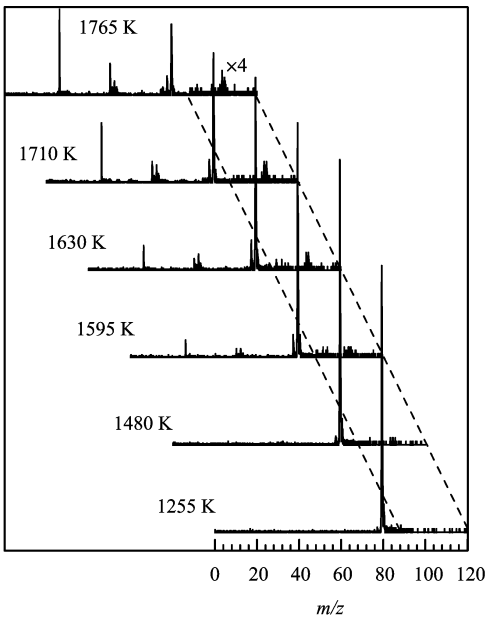

FIG. 1 The stack plot of photoionization mass spectra for the pyrolysis of pyridine with temperatures at the photon energy of 11.70 eV.

DOI:10.1088/1674-0068/22/02/204-209

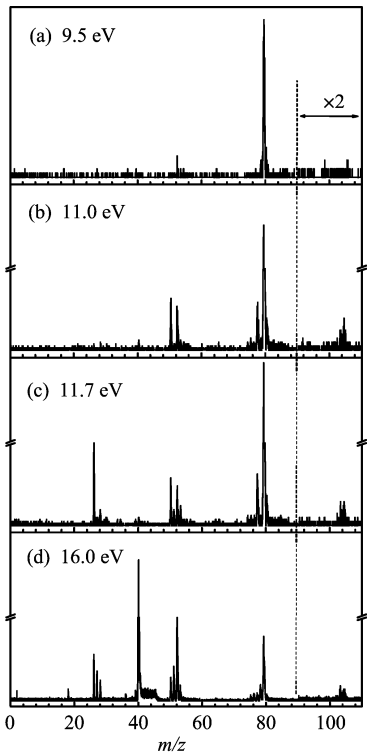

FIG. 2 Photoionization mass spectra of pyridine taken at 1745 K with different photon energies.

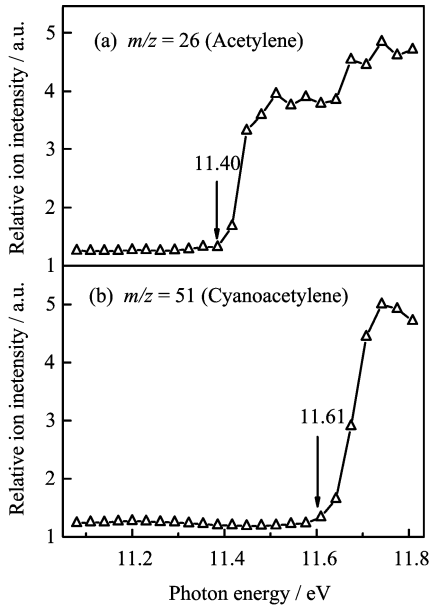

FIG. 3 PIE spectra measured in the pyrolysis of pyridine at the temperature of 1745 K.

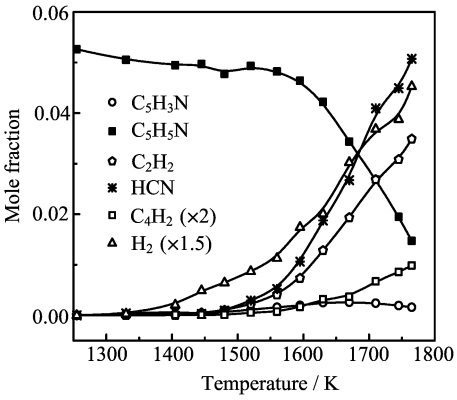

FIG. 4 Mole fraction profiles for the reactant (pyridine) and major products of the pyrolysis of pyridine.

intermediates and products are identified and listed in Table I.

B. Mole fraction profiles of pyrolysis species

The mole fractions of the observed pyrolysis species versus the temperature can be evaluated from the measurements of near-threshold photoionization mass spectra. The evaluation method of mole fraction has been reported in detail elsewhere [18]. It should be pointed out that the photoionization cross-section data of some nitrogenous compounds are not available, but fortunately, at the selected near-threshold photon energies they can be deduced from previous PIE measurements [15,20-25]. The mole fraction profiles of pyrolysis intermediates versus temperatures are shown in Fig.4 and Fig.5.

The mole fraction profiles of pyridine and major products are displayed in Fig.4. The mole fractions of C_2H_2, H_2, and the nitrogenous products HCN are of the magnitude order of 10^{-2}. The concentration of HCN increases continuously as the temperature increases with the highest yield. The initial formation temperatures (T_F) of C_2H_2 and HCN are around 1405 K which indicate they are not the primary product [10]. Lower concentration of C_5H_3N (cyanovinylacetylene) is detected with the T_F of 1255 K, which indicates C_5H_3N formed at the early stage of pyrolysis. The smallest molecule H_2 has the relative low T_F of 1330 K with abundant amount and its mole fraction increases monotonically. It is worth noting that no C_2H_3N was detected, which is in consistent with the previous results [10].

The mole fractions of most hydrocarbons, nitrogenous pyrolysis intermediates, and products are of the magnitude orders of 10^{-3} and 10^{-4}, as shown in Fig.5. The mole fraction profiles of intermediates including C_2H_4, C_4H_4, C_4H_5, C_6H_2, CH_4, and nitrogenous compounds vinylcyanide (C_3H_3N) and cyanoacetylene (C_3HN) are displayed in Fig.5(a). T_F values for C_4H_4 and C_3H_3N are 1405 K indicating they are the earliest formed species in Fig.5(a). Those products with T_F values of 1560 and 1630 K are produced in the secondary process. Figure 5(b) presents the mole fraction profiles of propyne (C_3H_4), C_4H_3, C_4H_6, cyanoallene (C_4H_3N) with the T_F in the range from 1440 K to 1520 K. Ben-

DOI:10.1088/1674-0068/22/02/204-209

TABLE I Intermediates and products identified in the pyrolysis of pyridine.

m/z	Formula	Species	IE/eV		X_M[b]	T_F[c]/K	T_M[d]/K
			Ref.[19]	This work[a]			
2	H_2	Hydrogen	15.43	15.43	3.02×10^{-2}	1330	1765
16	CH_4	Methane	12.61	12.60	7.17×10^{-4}	1595	1765
26	C_2H_2	Acetylene	11.40	11.40	3.49×10^{-2}	1405	1765
27	HCN	Hydrogen cyanide	13.60	13.60	5.07×10^{-2}	1405	1765
28	C_2H_4	Ethylene	10.51	10.51	1.13×10^{-3}	1480	1745
40	C_3H_4	Propyne	10.36	10.35	2.07×10^{-4}	1440	1765
50	C_4H_2	1,3-butadiyne	10.17	10.17	4.94×10^{-3}	1520	1765
51	C_3HN	Cyanoacetylene	11.62	11.61	6.58×10^{-4}	1480	1745
	C_4H_3	CH_3CCCH	8.02	8.08	1.47×10^{-4}	1520	1765
52	C_4H_4	Vinylacetylene	9.58	9.58	1.85×10^{-3}	1405	1710
53	C_3H_3N	Vinylcyanide	10.91	10.91	3.12×10^{-3}	1405	1745
	C_4H_5	CH_3CCCH_2	7.95 [35]	7.93	3.35×10^{-4}[e]	1560[f]	1670[f]
		CH_3CHCCH	7.97 [35]				
54	C_4H_6	1,3-butadiene	9.07	9.07	1.08×10^{-4}	1520	1710
65	C_4H_3N	Cyanoallene	10.35	10.37	8.38×10^{-5}	1560	1710
74	C_6H_2	1,3,5-hexatriyne	9.50	9.48	8.08×10^{-4}	1630	1765
77	C_5H_3N	Cyanovinylacetylene	9.33	9.33	2.59×10^{-3}	1255	1670
78	C_6H_6	Benzene	9.24		$<10^{-5}$	1255[g]	1670[g]
	C_5H_4N	Pyridyl radical	9.36				
79	C_5H_5N	Pyridine	9.26	9.26			
103	C_7H_5N	Benzonitrile	9.73	9.71	2.73×10^{-4}	1560	1710
104	$C_6H_4N_2$	3-pyridinecarbonitrile	10.10	9.96	3.25×10^{-4}	1560	1710

[a] The uncertainty for IE is 0.05 eV.
[b] The maximum mole fractions.
[c] T_F refers to the initial temperature for formation of species.
[d] T_M refers to the temperature relating to the maximum mole fraction.
[e] The value is total maximum mole fraction of CH_3CCCH_2 and CH_3CHCCH.
[f] The value is for both CH_3CCCH_2 and CH_3CHCCH.
[g] The value is for both benzene and pyridyl radical.

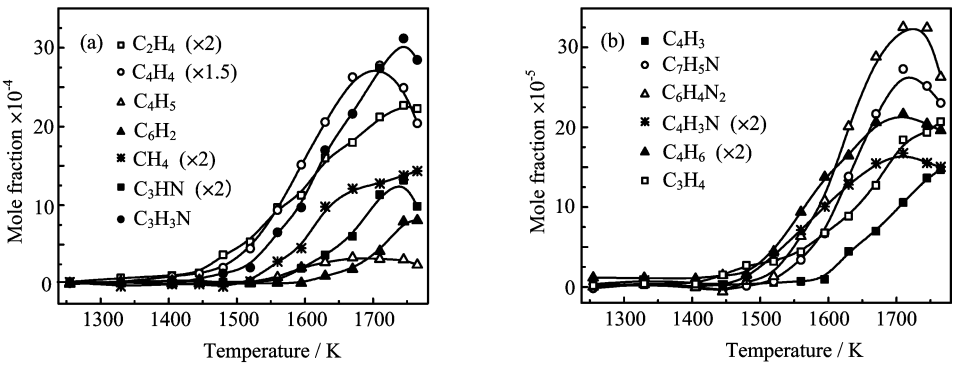

FIG. 5 Mole fraction profiles for the other pyrolysis intermediates and products formed from pyridine pyrolysis.

zonitrile (C_7H_5N) and 3-pyridinecarbonitrile ($C_6H_4N_2$) are the recombination products with high T_F values of 1560 K. The mole fraction profiles of most species in Fig.5 ascend to their highest values as temperature increases, except for those of CH_4 and C_4H_3.

C. Schematic reaction pathways

The reaction mechanism developed to interpret the above results involves a chain reaction initiated by C−H bond scission, as suggested in Refs.[13,14,26-29]. An es-

DOI:10.1088/1674-0068/22/02/204-209

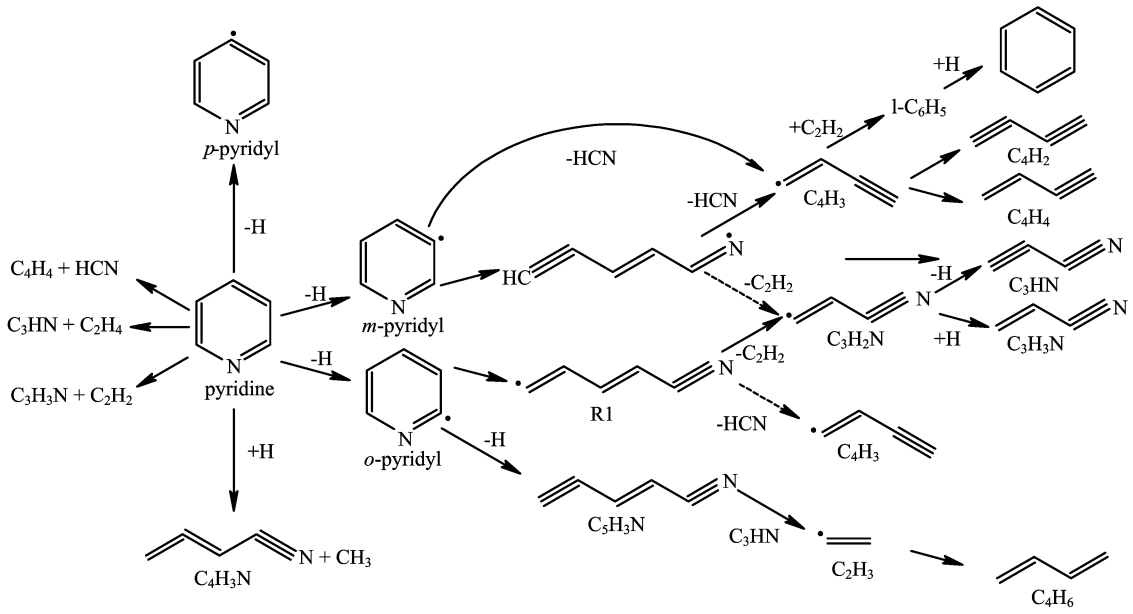

FIG. 6 A schematic decomposition pathways of pyridine pyrolysis at temperatures from 1255 K to 1765 K.

timation of the bond energies in the pyridine molecule would lead to the conclusion that the ring opening is less likely than C−H breakage [30]. The C−H and C−C bond energies in pyridine are the same as those in benzene, 428.0 and 489.9 kJ/mol, respectively, and the C−N bond energy is calculated to be 445.2 kJ/mol, supporting the conclusion that the C−H bond is more likely to be broken [10,12]. Thus the subsequent reactions are dependent on the thermochemistry of the cyclic pyridyl radicals produced by the scission of C−H bond. *o*-pyridyl, *p*-pyridyl, and *m*-pyridyl are the three possible C−H cleavage products which may all undergo ring opening. Among them *o*-pyridyl is unique in its ability to produce directly an open-chain cyano radical (CHCHCHCHCN, R1) [13,26].

Based on the assumption of the stability of R1, the dominant mechanism in the pyrolysis of pyridine at low temperature range is proposed to be the following [13]:

$C_5H_5N \rightarrow o\text{-},p\text{-},m\text{-}C_5H_4N\cdot + H\cdot$ (1)

$o\text{-}C_5H_4N\cdot \rightarrow R1$ (2)

$R1 \rightarrow C_2H_2 + \cdot HC{=}CHCN$ (3)

$H + C_5H_5N \rightarrow o\text{-},p\text{-},m\text{-}C_5H_4N\cdot + H_2$ (4)

The above short-chain mechanism is in accord with the experimental observations that C_5H_4N, C_2H_2, and C_3H_3N are the principal products at low temperature. C_2H_2 is the precursor for the formation of C_4H_2 and C_6H_2 by polymerization process [31]. Other than the major low-temperature chain mechanism, there is also a minor chain process which may arise via fission of a secondary H from R1, producing cyanovinylacetylene (CVA) [13].

$R1 \rightarrow HC{\equiv}C{-}CH{=}CHCN + H\cdot$ (5)

It is proposed that both pyridyl and open-chain radicals could undergo molecular elimination of HCN to produce the $C_4H_3\cdot$ radical as follows.

$o\text{-},p\text{-},m\text{-}C_5H_4N \rightarrow HCN + C_4H_3\cdot$ (6)

$R1 \rightarrow HCN + C_4H_3\cdot$ (7)

HCN is mainly deduced from the *m*-pyridyl and its subsequent open-ring radical [13,28]. Although the authors are unaware of any previous studies of HCN elimination from cyclic radicals, HCN elimination is an analogous process to the decomposition of benzyl radicals by invoking a rearrangement to a bicyclic $C_7H_7\cdot$ radical which can molecularly eliminate C_2H_2 [13]. The counterpart C_4H_3 radical is unstable and could readily form either C_4H_4 by H addition or C_4H_2 by H abstraction. Free radical and decomposition of unstable intermediates may attribute to the formation of minor reaction products. When C_3H_2N is formed, they may be consumed through different channels and produce C_3H_3N by H addition or C_3HN by H abstraction as described in Fig.6.

The *m*-pyridyl radical can also undergo a C_2H_3 radical elimination process together with the formation of C_3HN. It is possible that the recombination of the C_2H_3 radical may be slow due to the low concentration of the product 1,3-butadiene (C_4H_6). The direct ring opening of pyridine for the formation of HCN and C_4H_4, C_3HN and C_2H_4, C_3H_3N and C_4H_2 may also make potential contributions to the pyrolysis product. In the previous studies, the sooting tendency of pyridine decomposition has been reported to be substantially less than that of other aromatics (e.g. benzene) and even less than that of pyrrole [32,33]. The result of this investigation is consistent with the previous ones, since very few species with molecular weights higher than that of pyridine were observed [13]. Only mass 103 and 104 were found in this pyrolysis process. Mass 103 and mass 104 corre-

DOI:10.1088/1674-0068/22/02/204-209

spond to benzonitrile and 3-pyridinecarbonitrile which have also been identified in investigation of the low-pressure premixed pyridine rich flame [34]. Based on the present experimental results, it appears that it is also difficult to grow a second ring. The reason for this may be the short lifetime of the pyridyl radical. Another explanation relates to the relative reactivity of the carbon atoms on pyridine. Analogous to the growth mechanism for polyaromatic hydrocarbons, acetylene will add to the pyridyl radical. But the carbon atom located at meta position has the lowest reactivity and will inhibit the attraction of the additional second C_2H_2 needed for the ring formation [13,14]. The schematic decomposition pathways of pyridine pyrolysis at temperatures from 1400 K to 1845 K are summarized in Fig.6.

IV. CONCLUSION

The pyrolysis of pyridine was studied with tunable synchrotron VUV photoionization and molecular beam mass spectrometry. The evolution of the major and minor products in the pyrolytic process was imaged by both the temperature scanning profile and the energy scanning profile. The dominant pathways of the preferable open chain of *o*-pyridyl and *m*-pyridyl are presented schematically together with some free radical reactions accompanied by decomposition of unstable intermediates for the formation of minor products. Further analysis and theoretical calculation will be carried out to enrich the reaction network of the precursors for NO_x evolution.

V. ACKNOWLEDGMENTS

This work was supported by the Chinese Academy of Sciences, the Natural Science Foundation of China (No.20533040), the National Basic Research Program of China (973) (No.2007CB815204m), and the Ministry of Science and Technology of China (No.2007DFA61310).

[1] L. R. Snyder, Anal. Chem. **41**, 314 (1969).
[2] L. R. Synder, B. E. Buell, and H. E. Howard, Anal. Chem. **40**, 1303 (1968).
[3] C. F. Brandenburg and D. R. Latham, J. Chem. Eng. Data **13**, 391 (1968).
[4] D. K. Albert, Anal. Chem. **39**, 1113 (1967).
[5] J. A. Miller and C. T. Browman, Prog. Energy Combust. Sci. **15**, 287 (1989).
[6] A. E. Axworthy, V. H. Dayan, and G. B. Martin, Fuel **57**, 29 (1978).
[7] T. Kambara, T. Takarada, Y. Yamamoto, and K. Kato., Energy & Fuels **7**, 1013 (1993).
[8] J. C. Mackie, M. B. Colket, and P. F. Nelson, Int. J. Chem. Kinet. **23**, 733 (1991).
[9] P. F. Nelson, A. N. Buckley, and M. D. Kelly, Proc. Combust. Inst. **24**, 1259 (1992).
[10] T. J. Houser, M. E. McMarville, and T. Biftu, Int. J. Chem. Kinet. **12**, 555 (1980).
[11] C. D. Hurd and J. I. J. Simon, J. Am. Chem. Soc. **84**, 4519 (1962).
[12] H. I. Leidreiter and H. Gg. Z. Wagner, Phys. Chem. N. F. **153**, 99 (1987).
[13] J. C. Mackie, M. B. Colket, and P. F. Nelson, J. Phys. Chem. **94**, 4099 (1990).
[14] H. U. R. Memon, K. D. Bartle, J. M. Taylor, and A. Williams, Int. J. Energy Res. **24**, 1141 (2000).
[15] T. A. Cool, K. Nakajima, T. A. Mostefaoui, F. Qi, A. McIlroy, P. R. Westmoreland, M. E. Law, L. Poisson, D. S. Peterka, and M. Ahmed, J. Chem. Phys. **119**, 8356 (2003).
[16] T. A. Cool, K. Nakajima, C. A. Taatjes, A. McIlroy, P. R. Westmoreland, M. E. Law, and A. McIlroy, Proc. Combust. Inst. **30**, 1681 (2005).
[17] F. Qi, R. Y, B. Yang, C. Q. Huang, L. X. Wei, J. Wang, L. S. Sheng, and Y. W. Zhang, Rev. Sci. Instrum. **77** (2006).
[18] T. C. Zhang, J. Wang, T. Yuan, X. Hong, L. D. Zhang, and F. Qi, J. Phys. Chem. A **112**, 10487 (2008).
[19] P. J. Linstrom and W. G. Mallard, *NIST Chemistry Webbook*, In National Institute of Standard and Technology, (2005) (http://webbook.nist.gov/chemistry/).
[20] R. P. Thorn, P. S. Monks, L. J. Stief, S. C. Kuo, Z. Y. Zhang, S. K. Ross, and R. B. J. Klemm, J. Phys. Chem. A **102**, 846 (1998).
[21] J. Wirsich, Spectrosc. Lett. **23**, 741 (1990).
[22] D. M. Rider, G. W. Ray, E. J. Darland, and G. E. Leroi, J. Chem. Phys. **74**, 1652 (1981).
[23] M. Schwell, H. W. Jochims, H. Baumgartel, and S. Leach, Chem. Phys. **344** (2008).
[24] J. Kreile, H. D. Kurland, and W. S. Seibel, Chem. Phys. **155**, 99 (1991).
[25] N. Kanno and K. Tonokura, Appl. Spectrosc. **61**, 869 (2007).
[26] Y. Ninomiya, Z. B. Dong, Y. Suzuki, and J. Koketsu, Fuel **79**, 449 (2000).
[27] J. H. Kiefer, Q. Zhang, R. D. Kern, J. Yao, and B. Jursic, J. Phys. Chem. A **101**, 7061 (1997).
[28] J. K. Winkler, W. Karow, and P. Rademacher, J. Anal. Appl. Pyrolysis **4**, 576 (2000).
[29] N. R. Hore and D. K. Russell, J. Chem. Soc. Perkin Trans. II 269 (1998).
[30] M. J. S. Dewar, A. J. Harget, and N. Trinajstic, J. Am. Chem. Soc. **91**, 6321 (1969).
[31] R. E. Bandy, C. Lakshminarayan, R. K. Frost, and T. S. Zwier, J. Chem. Phys. **98**, 5362 (1993).
[32] S. W. Benson, F. R. Cruikshank, D. M. Golden, G. R. Huaugen, H. E. O'Neal, A. S. Rodgers, R. Shaw, and R. Walsh, Chem. Rev. **69**, 279 (1969).
[33] M. B. Colket, *in 21st Symp. (Int.) on Combustion*, Pittsburgh: Combustion Inst., 851 (1986).
[34] Z. Y. Tian, Y. Y. Li, T. C. Zhang, A. G. Zhu, and F. Qi, J. Phys. Chem. A **112**, 13549 (2008).
[35] N. Hansen, S. J. Klippenstein, C. A. Taatjes, J. A. Miller, J. Wang, T. A. Cool, B. Yang, L. X. Wei, C. Q. Huang, J. Wang, F. Qi, A. M. M. E. Law, and P. R. Westmorel, J. Phys. Chem. A **110**, 3670 (2006).

DOI:10.1088/1674-0068/22/02/204-209